Journal of Magnetics 17(3), 163-167 (2012) http://dx.doi.org/10.4283/JMAG.2012.17.3.163

Ab initio Study for Electronic Property and Ferromagnetism of (Cu, N, or F)-codoped ZnO

Byung-Sub Kang* and Kwang-Pyo Chae

Department of Nano Science and Mechanical Engineering, Konkuk University, Chungju 380-701, Korea

(Received 7 April 2012, Received in final form 14 September 2012, Accepted 15 September 2012)

The effects on the ferromagnetism of the O or Zn defect in Cu-doped ZnO with the concentration of 2.77-8.33% have been investigated by the first-principles calculations. The Cu doping in ZnO was calculated to be a kind of *p*-type ferromagnetic half-metals. When the Zn vacancy exists in Cu-doped ZnO, the Cu magnetic moment increases, while for the O vacancy it is reduced. It is noticeable that the ferromagnetic state was originated from the hybridized O(2p)-Cu(3d)-O(2p) chain formed through the *p-d* coupling. The carrier-mediated ferromagnetism by nitrogen or fluorine does not depend on their concentration.

Keywords : p-type ZnO, first-principles, vacancy, ferromagnetism

1. Introduction

Diluted magnetic semiconductors (DMSs) have attracted a great deal of attention because of the possibility of incorporating magnetic degree of freedom in traditional semiconductors [1-5]. DMS will play an important role in spintronics as semiconductors do in electronics. However, it is one of the primary challenges to create the ferromagnetic semiconductors due to the difficulty in the spin-injection into the semiconductors to form DMS at room temperature. Group II-VI semiconductors doped with 3d transition-metal (TM) show the ferromagnetism with high Curie temperature [6-8]. It seems that their band structures are suitable for the spin-injection. The stability of the ferromagnetic state and of a high Curie temperature in V-, Cr-, Fe-, Co-, or Ni-doped ZnO has been investigated theoretically [9]. For the 3d TM-doped ZnO, it is interested in their potential applications as spintronic devices within room-temperature ferromagnetism. In this paper, we have studied the electronic properties and the effects of O or Zn vacancy on the magnetic behavior in Cu-doped ZnO with a Cu concentration of 2.77-8.33%. The possibility of Cu as the nonmagnetic dopant to fabricate ZnO-based DMS is examined by the first-principles calculations. As it is well known, the defects and the impurities are believed to play important roles in DMSs of wide semiconductor gaps. We have already reported the effects on the electronic structure of the defect of Zn or O atom in V- or Mn-doped ZnO [10]. We have presented the results for the electronic properties and magnetism of Cu, N or F codoped ZnO under various dopant concentrations with (or without) the Zn or O vacancy.

*Corresponding author: Tel: +82-43-840-3627
Fax: +82-43-851-4169, e-mail: kangbs@kku.ac.kr

2. Computational Details

The first-principles calculations were performed using the full-potential linear muffin-tin orbital (FPLMTO) method [11] based on density functional theory. The muffin-tin radii of Cu, Zn, and O were chosen to be 2.2, 2.1, and 1.6 *a.u.*, respectively, with the plane-wave basis cutoff $|\mathbf{k}+\mathbf{G}|<4.1$ $a.u.^{-1}$ Brillouin zone integrations were performed with the special *k*-point method over a gamma-centered $4\times4\times4$ mesh. Using 64 *k* points of $4\times4\times4$ grid insured that the total energies and the magnetic moments were converged on a better 0.1 meV/cell and 0.01 μ_B/atom scale, respectively. For the exchange correlation functional, we employed both the local density approximation (LDA) and generalized gradient approximation (GGA) proposed by Janak-Moruzzi-Williams [12, 13].

The LMTO basis set and charge density were expanded in terms of the spherical harmonics up to $l = 6$ inside each muffin-tin sphere. The LMTO basis functions in the valence energy region were chosen as 4*s* and 3*d* for Cu, and 4*s*, 4*p*, and 3*d* for Zn. The basis function of Zn (or Cu) for the 4*s*, 4*p*, and 3*d* is generated with cut-off energy

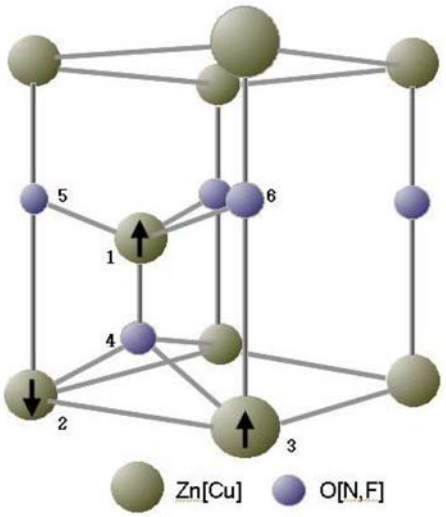

Fig. 1. (Color online) Wurtzite unit cell of ZnO with three Cu and N (or F) atoms. Number of 1, 2, or 3 denotes the substituted Cu atom, number of 4, 5, or 6 the substituted N or F sites. Up (or down) arrows represent the spins of Cu dopant. Their states denote an antiferromagnetic state.

of 223.04 eV (or 210.80 eV), 323.68 eV, and 474.64 eV (or 448.80 eV), respectively. The valence electrons were not assumed to have the spin-orbital coupling but had generated the self-consistent supercell potential by considering the scalar relativistic effects. The atomic potentials were approximated by spherically symmetric potential, however the full charge density including all non-spherical terms was evaluated by the Fourier transformation in the interstitial region. The electronic structure and magnetic properties on the Cu-doped wurtzite ZnO at the concentration of 2.77%, 5.55%, and 8.33% have been investigated for a supercell of 72 atoms with one, two, and three Zn atoms substituted by Cu. The wurtzite structure consists of Zn and O planes alternately stacked along the *c*-axis. The atomic structure of unit cell is displayed in Fig. 1.

3. Results and Discussion

We found that the calculated equilibrium lattice parameters are $a = 3.246$ Å, $c = 5.202$ Å, and internal parameters $u = 0.3819$ for the perfect ZnO. This value is the result by the GGA scheme. The calculated parameters are in agreement with the experimental ones [14-16]. The Cu dopant in ZnO is polarized ferromagnetically. The ferromagnetic (FM) state is more energetically favorable than the nonmagnetic and antiferromagnetic (AFM) states. The differences in total energy between the AFM and FM states are 76.1 meV and 66.5 meV for the Cu concentration of 5.55% and 8.33%, respectively. The Cu magnetic moment is nearly constant of 0.56 μ_B irrespective to the Cu concentration increases. The total magnetic moment in a supercell increases with respect to the Cu dopant increases. In comparison with the other result on the experimental work [17], the magnetic moment decreases as increasing the Cu concentration in Cu-doped ZnO thin films. The four O atoms coordinating the Cu dopant atom are spin polarized with a magnetic moment of 0.13 μ_B in parallel direction to the Cu atom. The results obtained by GGA are larger than that by LDA. These results are summarized in Table 1. When it is the substitution of Zn by Cu, the Cu dopant with O atom forms the O-Cu-O bond within the CuO_4 tetrahedron. It is formed the *p-d* coupling between the O 2*p* and Cu 3*d* electrons. Therefore, the ferromagnetism of Cu atom originates from the hybridized O(2p)-Cu(3d)-O(2p) chain. For $x = 0.0833$, a total magnetic moment per a supercell is 3 μ_B, that per Cu atom is 0.57 μ_B.

Table 1. Total energy difference between antiferromagnetic (AFM) and ferromagnetic (FM) states ($\Delta E = E_{total}$(AFM)$-E_{total}$(FM), in meV), the hole numbers of Cu (N_{Cu}, unit: *e*), the change of electron numbers in the interstitial regions with respect to the pure ZnO (N_{int}, unit: *e*). Magnetic moment (in μ_B) of a supercell, of Cu, in interstitial regions, of O sites, and of the nearest neighboring Zn site under the GGA and LDA calculations. The parentheses present the LDA result.

	$x = 0.0277$	$Zn_{1-x}Cu_xO$ $x = 0.0555$	$x = 0.0833$
ΔE	– (–)	76.1 (66.6)	66.5 (11.4)
N_{Cu}	1.22	1.23	1.24
N_{int}	1.08	1.89	2.11
Total	0.99 (0.95)	2.00 (1.91)	3.00 (2.67)
Cu	0.56 (0.55)	0.56 (0.56)	0.57 (0.49)
Interstitial	0.06 (0.11)	0.09 (0.33)	0.11 (0.49)
O (in CuO_4)	0.05 (0.01)	0.09 (0.07)	0.13 (0.08)
Other O	0.0 (0.0)	0.0 (0.0)	0.0 (0.0)
Zn	0.01 (0.0)	0.01 (0.0)	0.01 (0.0)

Table 2 summarizes the Cu magnetic moments in Cu-doped ZnO with the carrier of nitrogen or fluorine. The Cu magnetic moment with the increase of carrier concentration is reduced. As the F carrier concentration increases, the Cu 3d electrons become localized strongly so that the ferromagnetic state is reduced. Therefore the carrier-mediated ferromagnetism of Cu does not depend on the carrier concentration.

The Fig. 2 shows the density of states (DOS) for perfect $Zn_{1-x}Cu_xO$ at $x = 0.0277$, 0.0555, and 0.0833. The energy band by the Cu dopant shifts towards the lower-energy regions as compared to the bands of pure ZnO. The calculated band structures for the pure ZnO are in

Table 2. The Cu magnetic moments (in μ_B) in (Cu, N, or F)-codoped ZnO with the respect to carrier concentrations.

	$y = 0.0277$	$Zn_{1-x}Cu_xO_{1-y}X_y$ (X = N, F) $y = 0.0555$	$y = 0.0833$
	Hole (N)	doping	
2.77% Cu	0.67	0.57	0.34
5.55% Cu	0.46	0.48	0.24
	Electron (F)	doping	
2.77% Cu	0.17	0.11	0.0
5.55% Cu	0.37	0.19	0.0

agreement with those already calculated theoretically using the LDA [18] and GGA [10]. The amount of energy shift is about 0.19 eV for $x = 0.0277$. When the Cu concentration increases, the energy shifts do not occur. These configurations are a different trends to those for V or Mn dopant of other 3*d*-metal in ZnO [10]. When Cu is doped, the Zn state does not change nearly, while the O state changes at the regions of −4 eV and −2 eV. The O 2*p*-states move towards higher bonding region as increasing to the Cu concentration. The main-peak of O 2*s*-states locates around −17.5 eV are not included in this figure. The Cu 3*d*-states do not change nearly except upward shift of majority energy-band. It shows the character of half-metallicity up to the Cu concentration of 8.33%. The

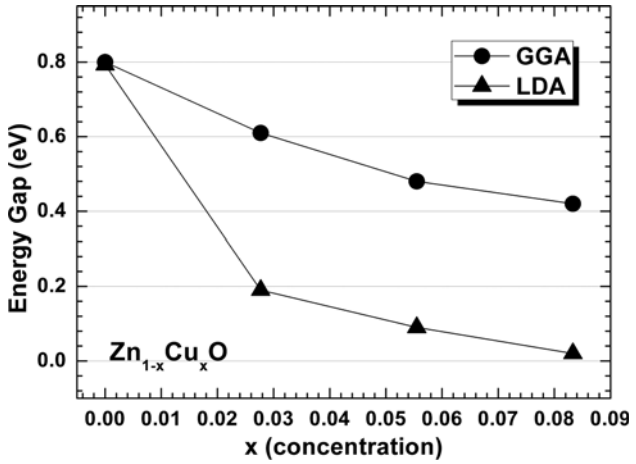

Fig. 3. Energy gap (half-metallic gap) for the FM states as a function of the Cu concentration in the complete Cu-doped ZnO with GGA and LDA calculations.

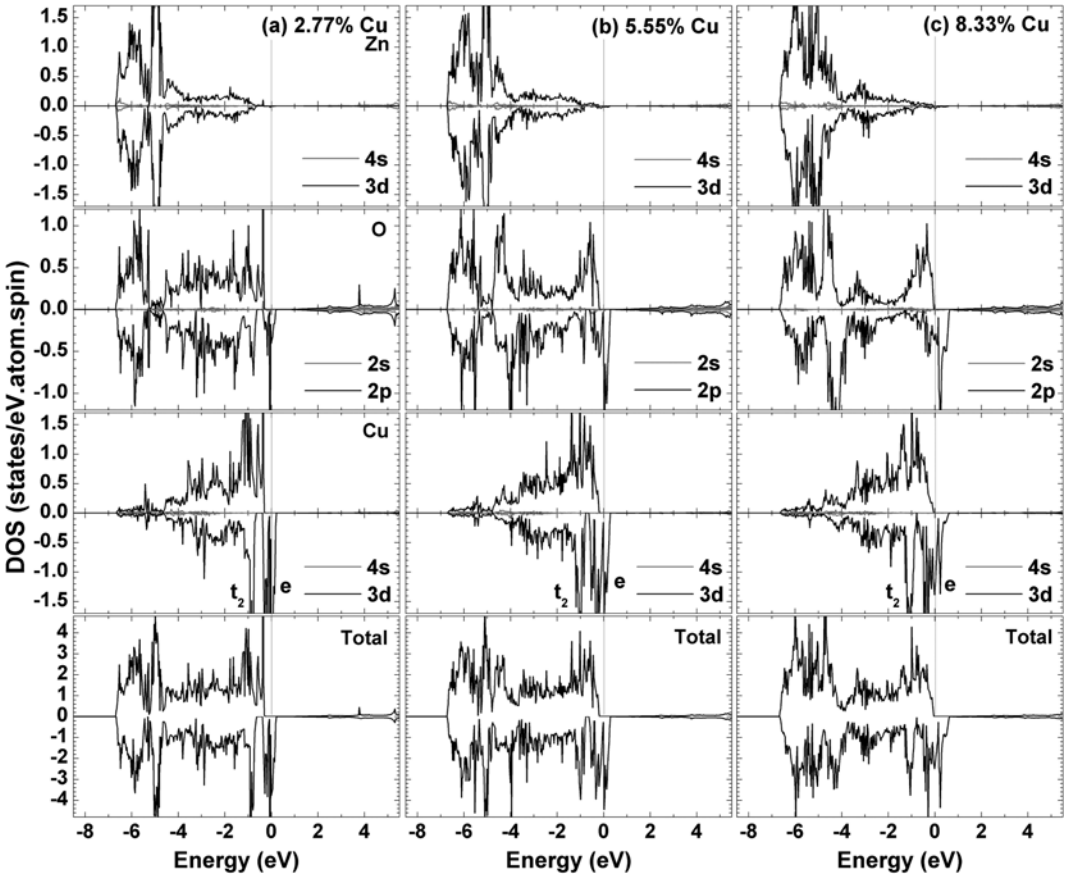

Fig. 2. DOS for Zn, O, and Cu sites in complete ZnO of FM under the GGA calculations within the Cu concentration of (a) 2.77%, (b) 5.55%, and (c) 8.33%. The E_F is set to zero (Solid-lines of gray).

lowest conduction band and the highest valence band originate mainly from Cu 3*d*- and O 2*p*-states as shown in Fig. 2.

For the Cu site in Cu-doped ZnO, the crystal field splitting between t_2 and *e*-states is strong. The Cu *e*-states are dominant and strongly localized at the Fermi level (E_F). The Cu t_2-states (d_{xy}) are located at the energy −1.0 eV below E_F. At lower Cu concentration, the *e*-states (d_{x2-y2}) in the minority band are localized. The interactions between the Cu *e*-state and O 2*p*-states become stronger as increasing to the Cu concentration.

The Zn 3*d*-states are located in the −4.5 eV to −6.5 eV regions below E_F. The Zn 4*s*-states are very small (there is not exist nearly). Therefore, the Zn^{2+} ion is chemically inactive. The bands near E_F are composed mostly of Cu 3*d*- and O 2*p*-states. These two states are hybridized strongly. The Cu and its coordinating four O atoms form a CuO_4 tetrahedron. This hybridization dominates the electronic and magnetic properties. As it can be seen in Fig. 2, the band structure of the FM Cu-doped ZnO below the Cu concentration of $x = 0.0833$ shows the half-metallic behavior with a half-metallic band-gap of 0.42 eV. That is, the majority-spin component is semiconducting while the minority-spin component is metallic, which has the E_F within the minority-spin band. There exists the energy gap in the majority spins. When the Cu atom exists in the complete ZnO, we call the half-metallic band-gap as the energy gap. The results on the energy gap as a function of the Cu concentration are displayed in Fig. 3.

Fig. 4 shows the DOS for $Zn_{1-x}Cu_xO$ at $x = 0.0277$. The O 2*p*-states just near the E_F induce the localized bands of occupied and unoccupied states. For $x = 0.0277$, the energy gap of 0.67 eV by the O vacancy is nearly same as compared with the complete Cu-doped ZnO, while for the vacancy of Zn atom it is larger by 0.79 eV. The half-metallic character disappears due to upward shift of the Cu dopant band. For a Zn vacancy, the E_F moves toward the top of valence band. Thus we can see the unoccupied band of majority spin-states.

When the vacancy of O atom is induced in Cu-doped ZnO, the Cu 3*d*-states do not change nearly, while the O 2*p*-states shift downward energy. The hybridization between the Cu 3*d*- and O 2*p*-states is reduced. The exchange interaction of these two sites becomes very weak. Thus the magnetization in a supercell becomes low due to the spin-polarization is weak. For an O vacancy of 2.77%, the magnetic moments of Cu and O atoms are 0.34 μ_B and 0.02 μ_B, respectively. For a Zn vacancy, the magnetic moments of Cu and O atoms are 0.65 μ_B and 0.12 μ_B, respectively. The magnetic moment of Cu-doped ZnO with

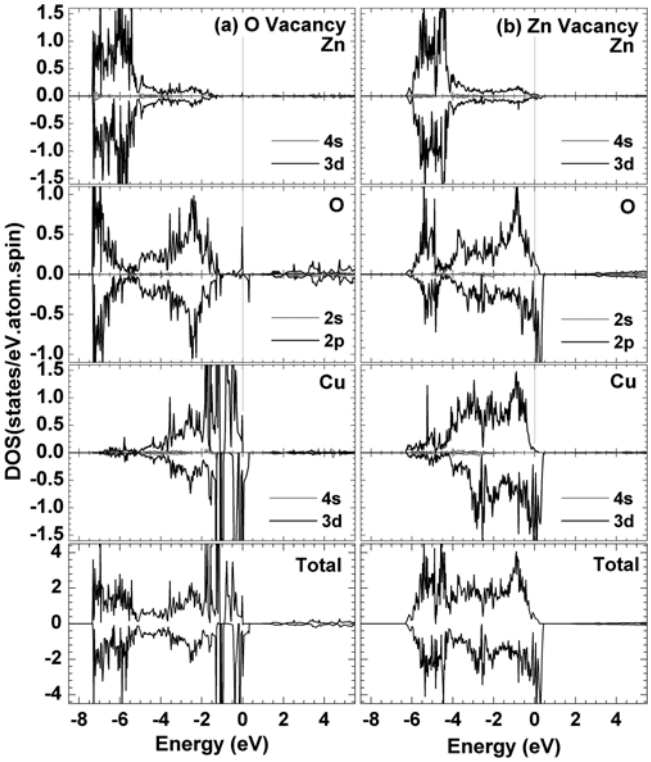

Fig. 4. Spin-dependent DOS for O, Zn, and Cu sites of $Zn_{0.9723}Cu_{0.0277}O$ (a) with the O vacancy of 2.77%, (b) with the Zn vacancy of 2.77%. The E_F is set to zero (Solid-line of gray).

O vacancy becomes lower than that with Zn vacancy. Even though the magnetic moment is small, it shows the ferromagnetism in wurtzite ZnO by the Cu doping. Therefore, the FM state of Cu dopant is very sensitive with respect to the defects of neighboring Zn or O cites.

The substitution of Zn by Cu atom is a *p*-type doping. We can count the net charge variation in the muffin-tin and in the interstitial regions. The hole-numbers are obtained by subtracting the number of electrons of Cu-doped ZnO from that of the pure ZnO. The charge redistribution mostly happens in the interstitial region or the site of vacancy instead of inside the muffin-tins. At higher Cu concentration, the number of electrons in Table 1 comes mainly from the O 2*p*-electrons. These electrons are not by the movement of Cu 3*d*-electrons. The hole-numbers of Cu are about 1.23 with respect to the Cu concentration. This indicates that the chemical valence of Cu is fractional and lies between 1+ and 2+ due to the strong Cu-O covalence. The Cu-O bond in Cu-doped ZnO is largely covalent because the strong hybridization between the Cu 3*d*- and O 2*p*-states in Fig. 2. Thus the Cu chemical valence is actually closer to 1+ than 2+. As can be seen in Table 1, there is no appreciable charge transfer between

two (or three) Cu atoms with the addition of the second (or the third) Cu to the supercell. The direct 3*d*-3*d* correlation between Cu atoms may be small because the variance of magnetic moment with respect to the Cu concentration does not change significantly. Therefore, the ferromagnetism of Cu dopant may be imply an indirect exchange mechanism by the vacancy of O or Zn site.

Conclusion

We have studied the magnetic and electronic properties for Cu-doped wurtzite ZnO by means of the first-principles calculations. In summary, the FM state of Cu-doped ZnO is more energetically stable than the AFM state. The total magnetic moments for 2.77%, 5.55%, and 8.33% Cu concentrations are about 1 μ_B, 2 μ_B, and 3 μ_B per supercell, respectively. The Cu magnetic moment is 0.56 μ_B with respect to the increasing of Cu concentration. When the carrier concentration is increased, the Cu 3*d*-states in ZnO are localized strongly, so that the Cu magnetic moment is reduced rapidly. The Cu-doped ZnO without the defect of O or Zn is a *p*-type. At higher Cu concentrations, the FM state is more stable than that of lower Cu concentrations. The Cu 3*d* and O 2*p* states in ZnO with Zn vacancy are strongly correlated. At this time, the Cu magnetic moment increases. However, when the O vacancy exists in Cu-doped ZnO, the Cu magnetic moment is strongly decreased because the hybridized O-Cu-O chain between the Cu 3*d*- and O 2*p*-states is reduced by the defect of O atom. The FM ground state in Cu-doped ZnO is very sensitive in the vacancy of Zn or O. These results imply that the copper is difficult to use as FM dopant in ZnO semiconductor. Avoiding the destruction of FM coupling of Cu dopant by the O vacancy site, detailed controlling O pressure should be very important factor to design the spintronic devices.

Acknowledgment

This work was supported by Konkuk University in 2012 (Dept. of Nano science and Mechanical engineering, Chungju).

References

[1] A. L. Rosa and R. Ahuja, Appl. Phys. Lett. **91**, 232109 (2007).
[2] Y. Chen, Q. Song, H. Yan, X. Yang, and T. Wei, Solid State Commun. **151**, 619 (2011).
[3] G. Yao, G. Fan, H. Xing, S. Zheng, J. Ma, S. Li, Y. Zhang, and M. He, Chem. Phys. Lett. **529**, 35 (2012).
[4] C. W. Zhang and S. S. Yan, J. Appl. Phys. **107**, 043913 (2010).
[5] P. Li, C. W. Zhang, J. Lian, S. Gao, and X. Wang, Solid State Commun. **151**, 1712 (2011).
[6] Y. Zheng, J. C. Boulliard, G. Y. Demaille, Y. Bernard, and J. F. Petroff, J. Cryst. Growth **274**, 156 (2005).
[7] C. H. Chien, S. H. Chiou, G. Y. Guo, and Y. D. Yao, J. Magn. Magn. Mater. **282**, 275 (2004).
[8] L.-H. Ye, A. J. Freeman, and B. Delley, Phys. Rev. B **73**, 033203 (2006).
[9] K. Sato and H. Katayama-Yoshida, Phys. Status Solidi B **229**, 673 (2002).
[10] B. S. Kang, W. C. Kim, Y. Y. Shong, and H. J. Kang, J. Cryst. Growth **287**, 74 (2006).
[11] S. Yu Savrasov, Phys. Rev. B**54**, 16470 (1996), and references therein.
[12] W. Kohn and L. I. Sham, Phys. Rev. **140**, B1133 (1965).
[13] J. P. Perdew, K. Burke, and M. Ernzerhof, Phys. Rev. Lett. **77**, 3865 (1996).
[14] B. G. Hyde and S. Andersson, Inorganic Crystal Structure, Wiley, New York (1989).
[15] A. Beltrán, J. Andrés, M. Calatayud, and J. B. L. Martins, Chem. Phys. Lett. **338**, 224 (2001).
[16] G. Y. Ahn, S.-L Park, I.-B. Shim, and C. S. Kim, J. Magn. Magn. Mater. **282**, 166 (2004).
[17] D. B. Buchhlz, R. P. H. Chang, J. H. Song, and J. B. Ketterson, Appl. Phys. Lett. **87**, 082504 (2005).
[18] P. Schröer, P. Krüger, and H. Pollmann, Phys. Rev. B **47**, 6971 (1993).